

Bladder tissue passive response to monotonic and cyclic loading

*Original*

Bladder tissue passive response to monotonic and cyclic loading / Zanetti, Elisabetta; M., Perrini; Bignardi, Cristina; Audenino, Alberto. - In: BIORHEOLOGY. - ISSN 0006-355X. - STAMPA. - 49:1(2012), pp. 49-63. [10.3233/BIR-2012-0604]

*Availability:*

This version is available at: 11583/2495982 since:

*Publisher:*

IOS Press

*Published*

DOI:10.3233/BIR-2012-0604

*Terms of use:*

This article is made available under terms and conditions as specified in the corresponding bibliographic description in the repository

*Publisher copyright*

(Article begins on next page)

## Bladder tissue passive response to monotonic and cyclic loading

Elisabetta M. Zanetti<sup>a</sup>, Michela Perrini<sup>b</sup>, Cristina Bignardi<sup>c</sup> and Alberto L. Audenino<sup>c<sup>✉</sup></sup>

<sup>a</sup>Department of Industrial Engineering, University of Perugia, Perugia, Italy

<sup>b</sup>Mechanical Engineering Department, Swiss Federal Institute of Technology, Zürich, CH

<sup>c</sup>Department of Mechanics, Politecnico di Torino, Torino, Italy

**Abstract.** The fundamental **passive** mechanical properties of the bladder need to be known in order to design the most appropriate long-term surgical repair procedures and develop materials for bladder reconstruction. This study has focused on the bladder tissue viscoelastic behavior, providing a comprehensive analysis of the effects of fibers orientation, strain rate and loading history. Whole bladders harvested from **one year old** fat pigs (**160 kg approximate weight**) were dissected along the apex-to-base direction and samples were isolated from the lateral region of the wall, as well as along apex-to-base and transverse directions. Uniaxial **monotonic** (stress relaxation) and **cyclic** tests at different frequencies have been performed with the Bose Electroforce<sup>®</sup> 3200. Normalized stress relaxation functions have been interpolated using a second order exponential series and loading and unloading stress-strain curves have been interpolated with a **non-linear** elastic model. The **passive** mechanical behavior of bladder tissue was shown to be heavily influenced by frequency and loading history, both in **monotonic** and cyclic tests. **The anisotropy of the tissue was evident in monotonic** and in **cyclic** tests as well, especially in tests performed on an exercised tissue and at high frequencies. In contrast, transverse and apex-to-base samples demonstrated an **analogous** relaxation behavior.

Key words: Dynamic, viscoelastic, stiffness, damping, relaxation, cycle number

Running Head: Bladder tissue response to loading history and frequency

### 1. Introduction

Different congenital or acquired pathologies (bladder exstrophy, neurogenic bladder

---

<sup>✉</sup>Address for correspondence: Alberto Audenino Department of Mechanical Engineering Politecnico di Torino Cso Duca degli Abruzzi 24 10129 Torino, Italy. Fax: +39 11 090-6999; E-mail: [alberto.audenino@polito.it](mailto:alberto.audenino@polito.it)

dysfunction, interstitial cystitis, bladder schistosomiasis, bladder cancer) determine anatomical and functional alterations of the bladder-sphincteric apparatus with consequent debilitating incontinence. It affects about 400 million people worldwide [13]. The characterization and quantification of the fundamental mechanical properties of a **healthy** bladder is mandatory in order to design the most appropriate long-term surgical repair procedures and to develop materials for bladder reconstruction.

**The bladder is a complex structure: it is made up of four tunics: mucosa, submucosa, muscularis and serous layers. The mucosal layer is the innermost tissue of the bladder and it is also known as the urothelium: it consists of from five to seven transitional epithelial cells layers which adapt their shape to the bladder replenishment. The submucosal layer, also known as the lamina propria, consists of blood, lymphatic vessels and nerves, within connective tissue and elastic fibers. It works as a sliding plane on which the tunica mucosa can change its aspect according to the bladder replenishment. The tunica muscularis is characterized by three layers of smooth muscular fibers that make the detrusor muscle. Even if theoretically divided, these layers penetrate each other. The serous coat is the parietal peritoneum, which only covers the upper region and the back-lateral faces of the bladder. The other parts of the bladder wall are covered by fatty-fibrous connective tissue.**

Side by side with the research in tissue engineering, different efforts have been made in order to optimize the pre-operative planning in reconstructive urology and diagnostics, taking advantage of methodologies which have already been tried in engineering and in other surgeries. The three-dimensional reconstruction of pelvic organs is a very useful tool both for diagnostic and therapeutic aims, as largely demonstrated in the literature. It makes it possible to perform minimally invasive surgery, to strengthen diagnostic capabilities and to evaluate different surgical options. With the passing of time, plane images have given place to 3D models, obtained through reverse engineering from CT or RM scans, leading to navigated surgery where the medical actor is constantly guided by a computer. Numerical models can

also make an important contribution to the pre-operative planning: for example, they make it possible to simulate different reconstructions and to evaluate the most suitable anchorage and constraints on the pelvis, according to applied loads [16]. Moreover, they have been applied to simulate prostatic volume variations during radiotherapy [11] or to perform fluid dynamic analyses of bladder-ureter systems [19].

The passage from a purely geometric model to a structural one can be accomplished if the mechanical properties of all materials are known, if the forces and pressures acting on the organs can be quantified, and if the boundary conditions are properly simulated [16]. In literature, many papers dealing with the mechanical characterization of bladder tissue can be found: Dahms et al. [6] worked on pig bladder tissue demonstrating that pig and human bladder tissues show similar mechanical behavior. They calculated elastic moduli in the collagen phase, having performed **monotonic** tests up to rupture, with specimens cut in the longitudinal direction. **As for the major part of biological tissues, the bladder wall shows a non-linear behavior and the physiologic range of deformation corresponds to the transition point of the stress-strain curve, between the elastin and collagen phases (100% - 200% strain according to Korossis et al. [13]).** The same authors [13] found how, in all regions, elastin appears to be oriented predominantly in the transverse (circumferential) direction. The histo-architecture of the bladder wall deeply affects its mechanical properties: in all regions, pig bladder tissue shows an increased compliance along the transverse direction (that is increased transition and failure strains, reduced collagen phase slopes), **whenever the collagen phase of the stress strain curve is being investigated.**

**In the literature, there is clinical evidence that the mechanical behavior of bladder is affected by its loading history, strain rate and loading duration: it has been found, for example, that an obstructed bladder extends, and lowers its compliance [12]. Other authors emphasized bladder fatigue in old compared to young patients [14]. The clinical assessment of bladder function is based on urodynamic parameters such as compliance, or the rate of**

reduction of vesical pressure at constant volume in stepwise cystometry. Since it is true that all observed behavior is the result of both the passive material properties and of functional data, it is the first of these that is being investigated here. At the same time, the role of cyclic loading in tissue engineering is being emphasized [4,8,15] as well as the importance of the proximity of the dynamic response of the engineered tissue to the dynamic response of the native one [2]. Yoo et al. [25] have given a comprehensive review of the most recent advances in tissue engineering with reference to the basic requirements to achieve functional tissues: proper scaffolds, a suitable environment and appropriate cells. The present paper contributes to the study of the mechanical properties of native tissues.

In dealing with the viscous features, the effect of strain rate has been studied in depth and reported in the literature [18]. Van Mastrigt et al. [23] derived an expression for the dependence of the viscoelastic response of bladder wall material on strain rate, in order to relate the results of measurements on strips of tissue to clinical measurements on the intact urinary bladder. The expression is based on a **non-linear** viscoelastic model, with elastic moduli depending exponentially on strain. The results show that relaxation constants are heavily influenced by the loading strain rate. Moreover, Coolsaet et al. [5] demonstrated that viscoelastic constants measured on tissue stripes derived from canine bladder are close to those obtained on the whole bladder. It is therefore plausible that these constants do not depend on specimen geometry.

In this work, **bladder tissue response to both monotonic and cyclic loading** have been **analyzed**, trying to establish a relationship between these behaviors and to assess if they are both affected by material anisotropy. Other relevant parameters **such as** frequency and the number of loading cycles (or loading history) have been here considered. According to the experimental tests, these parameters, which have often been overlooked, do have a major influence on the bladder tissue mechanical behavior.

## 2. Materials and methods

Six intact bladders of one year old fat pigs (160 kg approximate weight) were collected from a local abattoir, transported to the laboratory and frozen at  $-20^{\circ}\text{C}$ . Twenty four hours before testing, bladders were put into the fridge and, when completely defrosted, they were dissected along the apex-to-base line, as shown in Fig. 1a. Samples were harvested from the lateral region of the wall, as well as along the apex-to-base (AB) and transverse directions (T) (Fig. 1b). Specimens to be tested were isolated using a I-shaped die cutter, whose dimensions in mm are given in Fig. 2. Prior to testing, samples were measured by means of photogrammetry, taking two photos depicting the top and the lateral views of the bladder, together with a caliper. The recorded images were calibrated against the caliper in order to establish width and thickness profiles of the specimens, using the image analysis software ImageJ. The average width and thickness of samples used in this study were respectively  $4.66 \pm 0.72$  mm and  $3.99 \pm 1.04$  mm (mean  $\pm$  standard deviation). After their isolation, specimens were stored in the fridge within glass tubes containing PBS for less than 10 hours. The absence of calcium in the solution helped to ensure that the tissue was in an inactivated state and no spontaneous contraction would occur. During tests, performed at room temperature, samples were continuously dampened with the solution to keep them wet.

### 2.2. Mechanical characterization

The aim of the mechanical tests was to establish the effect of strain rate, orientation and loading history on the viscoelastic behavior of the bladder tissue. Therefore, both apex-to-base ( $n = 9$ ) and transverse ( $n = 16$ ) samples were subjected to cyclic and monotonic uniaxial tests. -Specimens were mounted onto the Bose Electroforce<sup>®</sup> by means of T/C Fatigue Grip-Titanium (Fig. 3). The position and the alignment of the sample were set by moving the crosshead (macro adjustments) and turning the cap screw located under the crosshead (micro

adjustments). Grips were well tightened, through lateral screws, to prevent sample slipping during tests. For all tests, a force threshold equal to 0.1 N has been applied as a reference point for zero-displacement. The test protocol provided a first test of stress relaxation followed by cyclic tests and a final test of stress relaxation.

The first and last relaxation tests were performed reaching a grip displacement of 12 mm (corresponding to an axial strain  $\epsilon \sim 100\%$  that is a physiologic strain level according to Korossis et al. [13]) with a rate of 0.16 mm/s (phase I), followed by a 600 s holding time (phase II). Cyclic tests (sinusoidal-wave loading) were performed at a grip displacement of  $3 \pm 3$  mm and in five steps, whose frequency and total number of cycles are reported in Table 1. The displacement range was limited by loading machine specifications (peak-to-peak tensile displacement  $< 12$  mm), and to prevent compressive loading of the specimen: this could take place as a consequence of stress relaxation.

During tests, load and displacement data were acquired respectively from the load cell (mounted on the fixed crosshead) and the linear differential transformer (LVDT). These signals were acquired at 0.03 mm displacement steps in the case of monotonic and 0.1 Hz, 0.5 Hz and 1 Hz cyclic tests, and at 0.003 mm displacement steps for 2 Hz and 5 Hz cyclic tests.

### 2.3. Analysis of results

Load (F) versus displacement (L) data were converted to stress and strain: the stress ( $\sigma$ ) was defined in the Lagrangian sense as the ratio of load to unloaded cross-sectional area, whereas the axial strain ( $\epsilon$ ) was defined as displacement referred to the initial specimen length (12 mm that is the distance between fixtures). Concerning the stress relaxation tests, phases I and II have been separately analyzed in order to evaluate the static stress-strain tissue behavior (I phase) and the relaxation tissue behavior (II phase).

As for phase I, the effects of loading history and orientation have been evaluated

considering the secant modulus  $E_s$  (slope of the chord connecting points at  $\epsilon = 0$  and  $\epsilon = 90\%$  in the stress-strain curve) both in the first test, and in the last test. In the first test,  $E_s$  practically agrees with the slope of the linear portion of the stress-strain curve ( $E$ ), while, after **cyclic** tests, the behavior of bladder tissue is anything but linear elastic, and it would be therefore meaningless to perform a linear regression. In phase II, the normalized stress relaxation functions were defined using the exponential series [1,20,24]:

$$\frac{\sigma(t)}{\sigma(0)} = \sum_{i=1}^{n_s} a_i e^{-t/\tau_i} \quad (1)$$

where  $\sigma(t)$  is the time dependent stress,  $\sigma(0)$  is the maximum stress value,  $a_i$  and  $\tau_i$  are the relaxation parameters,  $n_s$  is the series order, i.e. the number of exponential terms; in this work  $n_s = 2$  has been chosen on the basis of residuals analysis. In the **cyclic** tests, loading and unloading stress-strain curves have been separately interpolated with a **non-linear** elastic model:

$$\sigma = a \cdot e^{b\epsilon} \quad (2)$$

Differentiating with respect to  $\epsilon$ , the dynamic modulus could be defined as follows:

$$E_d = E_0 \cdot e^{b\epsilon} \quad (3)$$

as proposed by van Mastrigt et al. [23] for the bladder tissue. The effects of frequency, orientation and loading history have been evaluated considering three parameters: **the dynamic modulus limit as strain approaches zero,  $E_0$**  (Eq. 3), the dynamic modulus,  $E_{50}$ , at  $\epsilon = 50\%$ , and the specific damping  $h$ , defined as:

$$h = \frac{\text{loading area} - \text{unloading area}}{\text{mean area}} \quad (4)$$

All cited mechanical parameters underwent the Kolmogorov-Smirnov test in order to verify if they belonged to a normal distribution **despite having been obtained from different**



bladders. Since most tests gave positive results, it was possible to consider parameters as normally distributed, and the analysis of variance (ANOVA) could be applied.

As regards the stress relaxation tests, parameters from phase I and phase II were analyzed by two-way analysis of variance to investigate the significance of sample orientation (transverse and apex-to-base samples) and loading history (first and last test).

Parameters from cyclic tests were analyzed by three-way analysis of variance in order to identify the influence of sample orientation (transverse and apex-to-base samples), frequency (0.1, 0.5, 1, 2 and 5 Hz) and loading history (first and last cycle). Moreover, a further more detailed analysis was performed in order to identify which frequencies produced significantly different results according to the student's t-test. In all tests, the confidence level was set at 0.05.

### 3. Results

#### 3.1. Monotonic tests

Phases I and II of monotonic tests have been separately analyzed in order to evaluate the stress-strain tissue behavior (phase I) and the relaxation tissue behavior (phase II). Regarding phase I, the stress-strain curves for one transverse and apex-to-base samples, both for the first and the last test, have been plotted in Fig. 4 in order to examine the effect of loading history and directional anisotropy of the bladder wall. The mean secant moduli  $E_s$  are shown in Fig. 5.

Both groups demonstrated a linear stress-strain behavior during the first test, typical of soft tissues in this range of deformation (elastin phase). Loading history deeply affected the monotonic loading tissue response: stress-strain curves for the last test (after cyclic tests) are anything but linear elastic, with increasing slope at low deformations (tissue hardening) and decreasing slope at high deformations (the tissue seemed to yield). Specifically, last  $E_s$  test is

higher than first  $E_s$  test ( $p < 0.05$ , Table 2). Moreover, transverse samples were shown to be stiffer than apex-to-base ones both in the first and in the last test ( $p < 0.05$ , Table 2).

As for phase II, interpolated relaxation curves for transverse and apex-to-base samples are plotted in Fig. 6, both for the first and the last test. Model (1) fitted the experimental data well ( $R^2 > 0.98$ ). The tissue showed more pronounced stress relaxation following **cyclic** tests: the interpolating curve decreased faster after one similar initial steep slope (defined by the  $\tau_1$  time constant). The time constant,  $\tau_2$ , of the last test was, in fact, significantly lower than the constant  $\tau_2$  of the first test ( $p < 0.05$ , Table 2; Fig. 7).

In addition, transverse and apex-to-base samples demonstrated a similar relaxation behavior, with the differences between their respective time constants not statistically significant ( $p > 0.05$ , Table 2).

### 3.2. **Cyclic** tests

The tissue exhibited **non-linear** viscoelastic behavior typical of soft tissues and the model Eq. (2) fitted the experimental data well ( $R^2 > 0.98$ ). Loading stress-strain curves at all frequencies were characterized by a relative low stiffness “toe” region, which was nearly linear. Afterwards, the stress-strain curve showed a **non-linear** hardening pattern (Fig. 8). Moreover, the peak stress and the area bounded by the loading and unloading curves decreased **and stabilized** as the cycle number increased (Fig. 8).

$E_0$ ,  $E_{50}$  and  $h$  descriptive parameters are reported in Figs. 9, 10 and 11, respectively. The mechanical behavior of bladder tissue turned out to be heavily influenced by frequency. As can be seen in Fig. 12, the tissue became stiffer with increasing frequency (both  $E_0$ , and  $E_{50}$  significantly increased,  $p < 0.05$ , Table 3). The specific damping  $h$  also increased significantly ( $p < 0.05$ , Table 3). More specifically, the t-test at 95% confidence level revealed that parameter values at 0.1 Hz were significantly different with respect to all other frequencies. Moreover, the tissue mechanical behavior shifted from a nearly linear stress-

strain trend under static conditions (first monotonic test, Fig. 4) to a non-linear behavior under dynamic conditions (Fig. 12). Transverse and apex-to-base samples showed the same behavior at low strain ( $E_0$  values did not change significantly,  $p > 0.05$ , Table 3) but transverse samples were stiffer at high strain ( $E_{50}$  values differed significantly,  $p < 0.05$ , Table 3), especially at high frequencies. Concerning the energy dissipation, specific damping  $h$  did not appear to change in relation to specimen orientation ( $p > 0.05$ , Table 3): both sample groups were equally affected by frequency and fatigue.

Bladder tissue was affected by loading history, as shown in Fig 8. The stiffness at low strain,  $E_0$  decreased significantly with increasing number of cycles ( $p < 0.05$ , Table 3), while specific damping lowered as the cycle number increased and its influence changed in relation to loading frequency (Fig. 11, Table 3). On the contrary, loading history did not appear to have any influence on  $E_{50}$  values ( $p > 0.05$ , Table 3).

#### 4. Discussion

The objective of this study was to identify the effect of frequency, orientation, and loading history on the bladder tissue viscoelastic behavior. The effect of strain rate has been clearly demonstrated in the literature [18], but a systematic analysis of its influence had never been carried out on the bladder tissue, as it has on other soft tissues [7,17,22]. Seemingly, regional and directional anisotropy has been investigated only with reference to the static stress-strain behavior of bladder wall [13], while little is known about its viscoelastic properties. The effect of loading history has not yet been systematically investigated.

As for specimens, pig bladders have been investigated since other authors demonstrated that biomechanical and histological properties of human and pig bladder are very similar [6]. The I-shaped die cutter enabled the harvesting of samples with a quite constant and well defined shape (width =  $4.66 \pm 0.72$  mm), suitable for being gripped. This shape prevented specimen from over-stressing next to the grips, as witnessed by frequent failure in this area in

the case of constant section specimens [6]. Moreover, the small size of the specimens, similar to those in other published literature [7,13,17,22], allowed the tested tissue to be considered as homogeneous. Being highly deformable, specimens could not be measured with a caliper, and thus a photogrammetric method was chosen.

Testing protocol included storing specimens at  $-20^{\circ}\text{C}$ , as done also by other authors [6]. As illustrated in the following, results agree with finding of other researchers who simply stored the biological material at  $+4^{\circ}\text{C}$  and tested it within 48 h [10,13,18]; nevertheless, a systematic analysis of the effect of storage temperature on mechanical properties should be done.

Testing protocol did not include pre-conditioning cycles since the authors soon verified that bladder tissue mechanical behavior was heavily biased by the number of cycles carried out. Moreover, in these tests, samples have been continuously moistened with the PBS solution, but they were not dipped into the solution, as proposed by many authors [7,13,17]. This procedure permitted keeping the samples wet, avoiding dehydration, while still being able to appreciate the effect of specimen exudation (loss of liquid), as demonstrated by comparing tests carried out at different number of cycles.

The measured static elastic moduli agrees with results by Korossis et al. [13]. With regards to the directional anisotropy, in the deformation range investigated (0 - 90% that is a physiologic strain level according to Korossis et al. [13]), transverse samples were stiffer than apex-to-base ones because of the predominant orientation of elastin fibers (the load-bearing component at this strain level) in the transverse direction. Korossis et al. [13] found similar compliances in this range of deformation, while the same authors [13] and Gloeckner et al. [10] demonstrated that bladder tissue was more compliant in the transverse direction when a higher range of deformation was considered ('collagen' phase). On the contrary, the viscoelastic behavior of the bladder was shown not to depend on specimen orientation. This result agrees with Nagatomi's observations [18]. The bladder tissue exhibited a stress

relaxation behavior, typical of soft-tissues: the second order exponential series, widely used for describing the viscoelastic properties of soft tissues [1,20,24] fitted the experimental curves well in the time interval tested. However, it is evident that relaxation profiles have not completely leveled off (Fig. 6) and therefore a different model should perhaps be implemented to describe the undefined time behavior. Differences between apex-to-base and transverse sample parameters were not statistically significant ( $p > 0.05$ ). These phenomena, in fact, do not depend on the elastin fibers, which demonstrate low stress relaxation characteristics and negligible creep response [26]. They are related to collagen fibers, which show a significant amount of stress relaxation and creep [9] and are homogeneously distributed in the bladder tissue [13].

Concerning the cyclic tests, the selected frequencies range (0.1 to 5Hz) is of interest for tissue engineering [17]. The non-linear elastic exponential model, proposed by van Mastrigt et al. [23], fitted the stress-strain curves obtained in cyclic tests well, with  $R^2 = 0.99$ . All parameters significantly increased with increasing frequency ( $p < 0.05$ ) and this result was consistent with the histo-architecture of the bladder wall in the lateral region and, in particular, with the behavior of the elastin fibers. In fact, in the deformation range investigated (maximum = 50%), it was just elastin that conferred stiffness to the tissue and stored most of the strain energy [13]. At the higher frequencies,  $\alpha$ -helical segments of elastin stretch into a more extended conformation during the initial part of the stress-strain curve [21], thus stiffening the whole tissue. The results showed that tissue energy dissipation also depends on frequency: specific damping significantly increased with increasing frequency ( $p < 0.05$ ). The extended conformation of elastin fibers, in fact, enhances the internal friction between rearranged elastic fibers with viscous matrix interfibrillar connections, thus increasing energy dissipation at increasing frequencies [17].

Specimen loading history, taking place in the course of consecutive cycles, significantly affected the mechanical behavior of tissue. A comparison between the first and the last

relaxation test showed that in the latter the tissue exhibited a more pronounced relaxation and the stress-strain curves became nonlinear, with increasing stiffness at low deformations due to exudation, and decreasing stiffness at high deformations due to micro-failures. The influence of loading history should not lead us to think that permanent tissue damage has taken place: this is not possible at the strain levels investigated. More likely, it shows that the employed loading rate in cyclic tests has not allowed full tissue recovery, and in particular, has led to a poorer moisture content, and to temporary damage of those 'network connections' (attachments between elastin, protein and sugar molecules and the collagen) cited by Bischoff et al. [3] that can be disrupted during deformation, but might reform upon removal of the load if sufficient time is provided.

## 5. Conclusions

This study focused on the bladder tissue viscoelastic behavior providing a comprehensive analysis of the effects of loading history, orientation and strain rate. We found that loading history deeply affects both the monotonic and cyclic loading tissue response, stiffening the tissue under static conditions and emphasizing stress relaxation characteristics. Anisotropy was evident in static tissue behavior and in cyclic tests, especially on a fatigued tissue (last test) and at higher frequencies, when elastin fiber recruitment and stiffening occur. In contrast, transverse and apex-to-base samples demonstrated a similar relaxation behavior. The mechanical behavior of bladder tissue was also heavily influenced by frequency. The tissue got stiffer and dissipated more energy as frequency increased, especially in passing from 0.1 Hz to 0.5 Hz. Despite the variability of the experimental data, an analysis of variance could demonstrate the influence of loading history, orientation and strain rate on the mechanical properties of bladder tissue. Further studies will be carried out in order to link the passive mesoscale-tissue mechanical properties of the bladder wall, obtained from the uniaxial tests, with the mechanics of the whole bladder. The authors are developing a new

experimental set up to investigate the pressure-volume relationship during cystometric tests.

#### Acknowledgements

This work has been partially funded by the Italian Ministry of University and Research, (MIUR), PRIN2008 Program.

#### References

- [1] B. Ahn and J. Kim, Measurement and characterization of soft tissue behavior with surface deformation and force response under large deformations, *Med. Image Anal.* 14 (2010), 138-148.
- [2] S.C. Baker, G. Rohman, J. Southgate and N.R. Cameron, The relationship between the mechanical properties and cell behavior on PLGA and PCL scaffolds for bladder tissue engineering, *Biomaterials* 30 (2009), 1321-1328.
- [3] J.E. Bischoff, E.M. Arruda and K. Gosh, A rheological network model for the continuum anisotropic and viscoelastic behavior of soft tissue, *Biomech. Model Mechanobiol.* 3 (2004), 56–65.
- [4] S. Bouhout, R. Gauvin, L. Gibot, D. Aube' and S. Bolduc, Bladder substitute reconstructed in a physiological pressure environment, *J. Paediatr. Urology* 7 (2011), 276-282.
- [5] B.L. Coolsaet, W.A. van Duyl, R. van Mastrigt and J.W. Schouten, Viscoelastic properties of bladder wall strips, *Invest. Urol.* 12(1975), 351–355.
- [6] S.E. Dahms, H.J. Piechota, R. Dahiya, T.F. Lue and E.A. Tanagho EA, Composition and biomechanical properties of the bladder acellular matrix graft: comparative analysis in rat, pig and human, *Br. J. Urol.* 82 (1998), 411-419.
- [7] Z. Del Prete, S. Antonucci, A.H. Hoffman and P. Grigg, Viscoelastic properties of skin in Mov-13 and Tsk mice, *J. Biomech.* 37(2004), 1491-1497.
- [8] W.A. Farhat and H. Yeger, Does mechanical stimulation have any role in urinary

- bladder tissue engineering? *World J. Urol.* 26(2008), 301–305.
- [9] Y.C. Fung, *Biomechanics: Mechanical properties of living tissues*, Springer, New York, 1993, 568 pp.
- [10] D.C. Gloeckner, M.S. Sacks, M.O. Fraser, G.T. Somogyi, W.C. de Groat and M.B. Chancellor, Passive biaxial mechanical properties of the rat bladder wall after spinal cord injury, *J. Urol.* 167 (2002), 2247-2252.
- [11] N.D. James and S.A. Hussain, Molecular markers in bladder cancer, *Semin. Radiat. Oncol.* 15 (2005), 3-9.
- [12] Y.J. Kang, L.H. Jin, C.S. Park, H.Y. Shin, S.M. Yoon and T. Lee, Early sequential changes in bladder function after partial bladder outlet obstruction in awake sprague-dawley rats: focus on the decompensated bladder, *Korean J. Urol.* 52 (2011), 835-841.
- [13] S. Korossis, F. Bolland, J. Southgate, E. Ingham and J. Fisher J, Regional biomechanical and histological characterization of the passive porcine urinary bladder: implication for augmentation and tissue engineering strategies, *Biomaterials* 30 (2009), 266–275.
- [14] A.T. Lin, C.H. Yang and L.S. Chang, Impact of aging on rat urinary bladder fatigue, *J. Urol.* 157 (1997), 1990-1994.
- [15] R. Long Heise, J. Ivanova, A. Parekh, and M.S. Sacks, Generating elastin-rich small intestinal submucosa-based smooth muscle constructs utilizing exogenous growth factors and cyclic mechanical stimulation, *Tissue Eng. Part A* 15 (2009), 3951–3960.
- [16] G. Marino and C. Bignardi C, Reconstruction, application and evaluation of a finite element method to study the pelvic floor. Preliminary results, *Minerva Urol. Nefrol.* 54 (2002), 183-187.
- [17] D. Mavrilas, E.A. Sinuoris, D.H. Vynios and N Papageorgakopoulou, Dynamic mechanical characteristics of intact and structurally modified bovine pericardial



- tissues, *J. Biomech.* 38 (2005), 761-768.
- [18] J. Nagatomi, K.K. Toosi, M.B. Chancellor and M.S. Sacks, Contribution of the extracellular matrix to the viscoelastic behavior of the urinary bladder wall, *Biomech. Model Mechanobiol.* 7 (2008), 395-404.
- [19] J.J. Pel and R. van Mastrigt, Development of a CFD urethral model to study flow-generated vortices under different conditions of prostatic obstruction, *Physiol. Meas.* 28 (2007), 13-23.
- [20] D.P. Pioletti and L.R. Rakotomanana, Non linear viscoelastic laws for soft biological tissues, *Euro. J. Mech. A Solids* 19 (2000), 749-759.
- [21] F.H. Silver, G.P. Seehra, J.W. Freeman and D. DeVore, Viscoelastic properties of young and old human dermis: A proposed molecular mechanism for elastic energy storage in collagen and elastin, *J. Appl. Polym. Sci.* 86 (2002), 1978-1985.
- [22] J.G. Snedeker, F.R. Niederer, F.R. Schmidlin, M. Farshad, C.K. Demetropoulos, J.B. Lee and K.H. Yang, Strain-rate dependent material properties of the porcine and human kidney capsule, *J. Biomech.* 38 (2005), 1011-1021.
- [23] R. Van Mastrigt, and J.C. Nagtegaal, Dependence of the viscoelastic response of the urinary bladder wall on strain rate, *Med. Biol. Eng. Comput.* 19 (1981), 291-296.
- [24] J.Z. Wu, R.G. Dong, W.P. Smutz and A.W. Schopper, Modeling of time-dependent force response of fingertip to dynamic loading, *J. Biomech.* 36 (2003), 383-392.
- [25] J.J. Yoo, J. Olson, A. Atala and B. Kim, Regenerative Medicine Strategies for Treating Neurogenic Bladder, *Int. Neurourol. J.* 15 (2011), 109-119.
- [26] Y. Zou Y and Y. Zhang, The orthotropic viscoelastic behavior of aortic elastin, *Biomech. Model Mechanobiol.* 10 (2011), 613-625.

Tables

Table 1. Cyclic tests: frequency and number of cycles for each consecutive step

Step	Frequency, Hz	No. of cycles
1	0.1	30
2	0.5	30
3	1.0	50
4	2.0	60
5	5.0	100

Table 2. Anova results for **monotonic** tests: p values. Numbers in boldface type point to which parameters **or interaction of factors** produced significant differences,  $p < 0.05$ .

Parameter	Orientation	Fatigue	Fatigue Orientation
$E_s$ (MPa)	0.001	<0.001	0.148
$\tau_{1_s}$ (s)	0.799	0.500	0.196
$\tau_{2_s}$ (s)	0.800	0.008	0.333

Table 3. Anova results for cyclic tests: p values. Numbers in boldface type point to which factors or interaction of factors produced significant differences,  $p < 0.05$ .

Factor(s)	Frequency	Orientation	Loading history	Frequency: Orientation	Frequency: Loading history	Orientation: Loading history	Frequency: Orientation: Loading history
$E_0$ , MPa	0.001	0.148	<0.001	0.887	0.058	0.416	0.952
$E_{50}$ , MPa	0.001	0.002	0.110	0.487	0.960	0.927	0.422
h, Eq. 4	<0.001	0.200	0.020	0.492	<0.001	0.890	0.921

## Figure Legends

Fig. 1. Bladder dissection and sample localization. Left: whole bladder in the anterior-posterior view and dissection plane connecting the urethra's opening to the bladder's apex. Right: cut-opened bladder showing the map of anatomical regions.

Fig. 2. I-shaped specimen (numbers refer to mm distances): the calibrated specimen length is equal to 12 mm, while its calibrated width is equal to 5 mm; samples have been cut dipping the sharp-edged cutter into the opened and flattened bladder.

Fig. 3. Sample mounted onto the Bose Electroforce<sup>®</sup> by means of T/C Fatigue Grips-Titanium. A: crosshead; B: load cell; C: grips; D: screws; E: sample; F fixtures.

Fig. 4. Monotonic first and last test stress-strain curves in phase I for two samples: transverse orientation (T) – solid lines; apex-to-base orientation (AB) – dashed lines; a, b, c, d are chords connecting points at  $\epsilon = 0$  and  $\epsilon = 90\%$ ; their slope corresponds to the secant modulus  $E_s$ .

Fig. 5. Monotonic first and last test results showing the mean values of the secant modulus,  $E_{sT}$  at the two orientations. The bars represent one standard deviation of the average value.

Fig. 6. Mean fitted relaxation curves in Phase II after monotonic tests at transverse (T - solid lines), and apex-to-base (AB - dashed lines) orientations.

Fig. 7. Mean values  $\pm$  s.d. of the time constants  $\tau_1$  (left) and  $\tau_2$  (right) in Phase II at first and last monotonic tests. Only  $\tau_2$  is significantly lower at the last test than at the first test.

Fig. 8. Cyclic tests (1 Hz): stress-strain curve of one sample at the 1st, 10th, 20th, 30th, 40th and 50th cycle. The peak stress and the area bounded by the loading and unloading curves decreased and stabilized as the cycles number increased.

Fig. 9. Mean values  $\pm$  s.d of the dynamic modulus at low strain  $E_0$  in cyclic tests in the transverse (upward diagonal pattern) and apex-to-base (outlined diamond pattern) orientations, obtained in the 1<sup>st</sup> cycle (dark background) or in the last cycle (light background).  $E_0$  is not significantly affected by sample orientation; it is higher at higher

frequencies and it diminishes at increasing number of cycles.

Fig. 10. Mean values  $\pm$  s.d of the dynamic modulus,  $E_{50}$ , at 50% strain in cyclic tests in the transverse (upward diagonal pattern) and apex-to-base (outlined diamond pattern) orientations, obtained in the 1<sup>st</sup> cycle (dark background) or in the last cycle (light background).  $E_{50}$  is higher in the transverse orientation and at higher frequencies and is not significantly affected by loading history.

Fig. 11. Mean values  $\pm$  s.d of the specific damping in cyclic tests in the transverse (upward diagonal pattern) and apex-to-base (outlined diamond pattern) orientations, obtained in the 1<sup>st</sup> cycle (dark background) or in the last cycle (light background).  $h$  is not affected by sample orientation; it is lower at higher frequencies and it diminishes at increasing number of cycles.

Fig. 12. Cyclic tests: fitted stress-strain loading curves of the first cycle at 0.1, 0.5, 1, 2, 5 Hz for one sample.

Figure 1

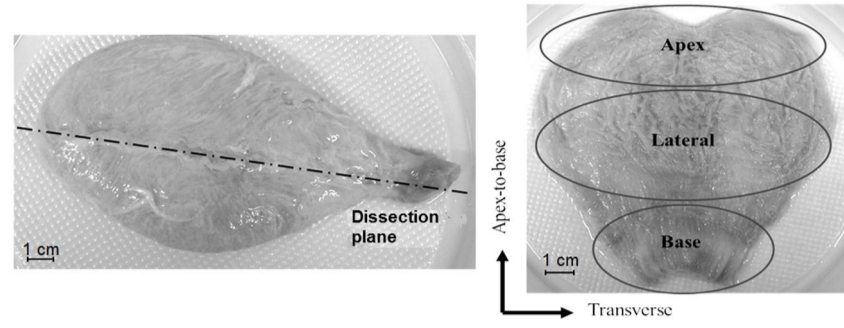


Figure 2

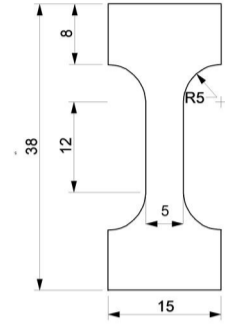


Figure 3

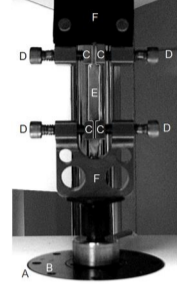


Figure 4

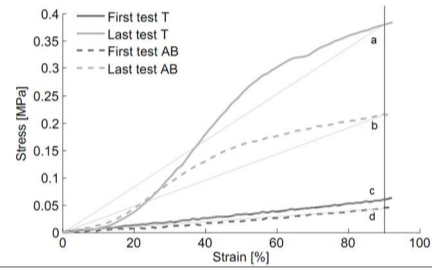


Figure 5

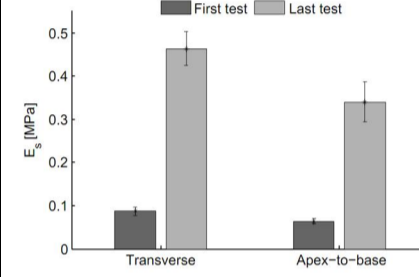


Figure 6

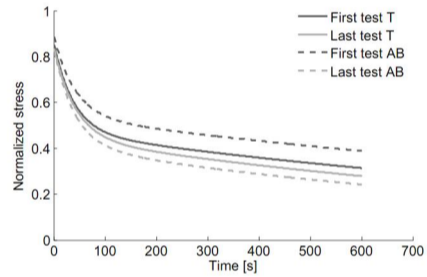


Figure 7

